online data

Oxidation of heparan sulphate by hypochlorite: role of N-chloro derivatives and dichloramine-dependent fragmentation

Martin D. REES, David I. PATTISON and Michael J. DAVIES[1]

Free Radical Group, Heart Research Institute, Camperdown, Sydney, NSW 2050, Australia

Activated phagocytes release the haem enzyme MPO (myeloperoxidase) and produce superoxide radicals and H_2O_2 via an oxidative burst. MPO uses H_2O_2 and Cl^- to form HOCl, the physiological mixture of hypochlorous acid and its anion present at pH 7.4. As MPO binds to glycosaminoglycans, oxidation of extracellular matrix and cell surfaces by HOCl may be localized to these materials. However, the reactions of HOCl with glycosaminoglycans are poorly characterized. The GlcNAc (*N*-acetylglucosamine), $GlcNSO_3$ (glucosamine-*N*-sulphate) and $GlcNH_2$ [(N-unsubstituted) glucosamine] residues of heparan sulphate are potential targets for HOCl. It is shown here that HOCl reacts with each of these residues to generate N-chloro derivatives, and the absolute rate constants for these reactions have been determined. Reaction at $GlcNH_2$ residues yields chloramines and, subsequently, dichloramines with markedly slower rates, $k_2 \sim 3.1 \times 10^5$ and $9\ M^{-1} \cdot s^{-1}$ (at 37 °C) respectively. Reaction at $GlcNSO_3$ and GlcNAc residues yields N-chlorosulphonamides and chloramides with $k_2 \sim 0.05$ and $0.01\ M^{-1} \cdot s^{-1}$ (at 37 °C) respectively. The corresponding monosaccharides display a similar pattern of reactivity. Decay of the polymer-derived chloramines, N-chlorosulphonamides and chloramides is slow at 37 °C and does not result in major structural changes. In contrast, dichloramine decay is rapid at 37 °C and results in fragmentation of the polymer backbone. Computational modelling of the reaction of HOCl with heparan sulphate proteoglycans (glypican-1 and perlecan) predicts that the $GlcNH_2$ residues of heparan sulphate are major sites of attack. These results suggest that HOCl may be an important mediator of damage to glycosaminoglycans and proteoglycans at inflammatory foci.

Key words: glycosaminoglycan, heparan sulphate, heparin, hypochlorite, myeloperoxidase, oxidation.

INTRODUCTION

Activated phagocytes release the haem enzyme MPO (myeloperoxidase) and produce high concentrations of the superoxide anion ($O_2^{\bullet -}$) and its dismutation product H_2O_2 via an oxidative burst. MPO reacts with H_2O_2 and Cl^- to form a mixture of hypochlorous acid and its anion hypochlorite ($HOCl/^-OCl$, pK_a 7.59; this mixture is henceforth referred to as HOCl) [1]. MPO is a highly basic protein and is known to bind, via electrostatic interactions, to negatively charged materials such as the polyanionic glycosaminoglycans [both HA (hyaluronan) and those of proteoglycans] of extracellular matrix and those present on cell surfaces [2].

Localized excess production of HOCl has been implicated in a number of diseases that involve an acute or chronic inflammatory response (e.g. atherosclerosis, rheumatoid arthritis and asthma) [3]. Both active MPO, and products of its action (such as 3-chloro-Tyr generated from reaction of HOCl with protein tyrosine residues), have been detected in human atherosclerotic lesions [4], diseased human kidneys [5] and at other sites of chronic inflammation. MPO levels have also been shown to be positively associated with coronary artery disease, and to be predictive of future cardiac events [6]. The binding of MPO to matrix components and cell-surface glycosaminoglycans would be expected to direct MPO-mediated oxidative damage towards this material; this has been observed in some cases [2,7,8]. HOCl damage to extracellular matrix in human atherosclerotic lesions and the glomeruli of human kidneys has also been identified using monoclonal antibodies [9,10] and product analysis [8].

Degradation of glycosaminoglycan and extracellular matrix has been postulated to play a key role in a number of inflammatory diseases [11,12], and the fragments that this damage would liberate have been shown to have potent biological effects (e.g. [13,14]). Whether the degradation of glycosaminoglycans at sites of chronic inflammation occurs via enzyme-mediated reactions (e.g. via the action of heparanase or hyaluronidases) or via the action of oxidants such as HOCl is currently unknown.

Extensive studies have been conducted *in vitro* on the reactions of HOCl with isolated cell components including proteins, lipids and antioxidants, and the products of some of these reactions have been elucidated (reviewed in [15]). Absolute rate constants have been reported for the reactions of HOCl with potential reactive sites on these species [16–19]. Based on these kinetic data, computational models of the reaction of HOCl with proteins and lipoproteins have been created; these models are of value in predicting the structural consequences of these reactions [16,17].

Reactions of HOCl with glycosaminoglycans are much less well characterized. Glycosaminoglycans are high molecular mass, linear polysaccharides that are composed of repeating disaccharide units that contain a glycosamine residue. The glycosamine residues in HA, chondroitin sulphate, dermatan sulphate and keratan sulphate (glucosamine and galactosamine) are exclusively N-acetylated. It has been shown that HOCl can induce site-specific damage to HA and chondroitin sulphates by reaction with the amide (N-acetyl) groups present on these polymers [20–22]. Reaction with these sites generates chloramides (R-NCl-C(O)-CH_3) that are readily reduced to nitrogen-centred (amidyl) radicals

Abbreviations used: b-HP, bovine lung heparin; dnsp-HP, partially de-N-sulphated porcine intestine heparin; GlcNAc, *N*-acetylglucosamine; $GlcNH_2$, (N-unsubstituted) glucosamine; $GlcNSO_3$, glucosamine-*N*-sulphate; HA, hyaluronan; MPO, myeloperoxidase; p-HP, porcine intestine heparin; p-HS, porcine intestine heparan sulphate; TNB, 5-thio-2-nitrobenzoic acid.

[1] To whom correspondence should be addressed (email m.davies@hri.org.au).

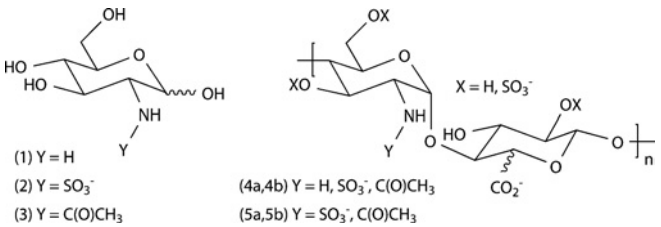

Figure 1 Glycosamine monosaccharides and glycosaminoglycans

(1) $GlcNH_2$, (2) $GlcNSO_3$, (3) GlcNAc, (4a) p-HS, (4b) dnsp-HP, (5a) p-HP and (5b) b-HP. It should be noted that the free amino groups of $GlcNH_2$ residues are protonated ($R\text{-}NH_3^+$) at physiological pH and that the polymer-derived uronic acid residues are β-D-glucuronic acid or α-L-iduronic acid. The repeat unit structures shown do not represent low energy conformations. Polymer residue abundance/substitution data is given in Table 1.

by redox-active metal ions or superoxide radicals [20–22]. Subsequent rearrangement reactions of these nitrogen-centred radicals can give rise to carbon-centred species, cleavage of the glycosidic linkages, and hence fragmentation of the polymers [20–22]. Little is known, however, regarding the reaction of HOCl with heparan sulphate and the closely related polymer heparin. Both polymers contain GlcNAc (*N*-acetylglucosamine) residues and $GlcNSO_3$ (glucosamine-*N*-sulphate) residues in differing proportions; heparan sulphate can also contain $GlcNH_2$ [(N-unsubstituted) glucosamine] residues (Figure 1). The $GlcNSO_3$ sulphonamide groups and the $GlcNH_2$ amine groups might be expected to react more rapidly with HOCl than the GlcNAc amide groups (e.g. the rate constants for the reaction of HOCl with free amine and amide groups in proteins [17]). The nature of the products formed in these reactions (presumed to be N-chloro derivatives) and their stability are poorly defined. The aim of the present study was therefore to determine absolute rate constants for the reactions of HOCl with the glycosamine residues present in heparan sulphate and heparin and to investigate the nature of the species formed, their stability and their possible involvement in polymer fragmentation. These data are important in understanding the fate of HOCl generated at inflammatory foci and the consequences of this oxidant production.

EXPERIMENTAL

Materials

Solutions were prepared using water filtered through a four-stage Milli Q system. pH control was achieved using 0.1 M phosphate buffer (pH 7.4) treated with washed Chelex resin (Bio-Rad, Hercules, CA, U.S.A.) to remove contaminating metal ions. b-HP (bovine lung heparin), p-HP (porcine intestinal heparin) and D-glucosamine hydrochloride were from Sigma (St. Louis, MO, U.S.A.). dnsp-HP (partially de-N-sulphated porcine intestine heparin) and p-HS (porcine intestine heparan sulphate) were from Celsus Laboratories (Cincinnati, OH, U.S.A.). HA (sodium salt, 120 kDa) was from Genzyme (Cambridge, MA, U.S.A.). GlcNAc was from Toronto Research Chemicals (North York, ON, Canada). $GlcNSO_3$ and heparin octasaccharides (obtained by heparinase I cleavage of heparin and isolation by gel permeation chromatography) were from Dextra Laboratories (Reading, U.K.). HOCl solutions were prepared by dilution of a concentrated stock [0.5 M in 0.1 M NaOH; standardized spectrophotometrically at pH 12 using a molar absorption coefficient ε_{292} ($^-$OCl) 350 $M^{-1} \cdot cm^{-1}$] into 0.1 M phosphate buffer (pH 7.4). All other chemicals were of analytical grade.

UV–visible spectroscopy and stopped-flow studies

Kinetic studies were carried out (relative to a 0.1 M phosphate buffer, pH 7.4, baseline) using an Applied Photophysics SX.18MV stopped-flow system (2.5 ms to 10 s timescale), or a PerkinElmer Lambda 40 UV–visible spectrometer either with (5–900 s timescale) or without (>15 min timescale) a Hi-Tech SFA 20 stopped-flow attachment as described previously [16,17]. Temperature control was achieved using circulating water from a thermostatically maintained water bath (both stopped-flow systems at 10, 22 and 37 °C) and/or a cuvette holder thermostatically maintained by means of a Peltier block (Hi Tech stopped-flow system and spectrometer alone at 22 and 37 °C).

For kinetic experiments using the monosaccharides, HOCl was kept as the limiting reagent with > 2.5-fold excess of substrate. This limits secondary reactions, and at high substrate excesses reduced the kinetics to pseudo first order. To obtain second-order rate constants, time-dependent UV–visible spectral data were imported into Specfit software (version 3.0.15, Spectrum Software Associates, Chapel Hill, NC, U.S.A.; see http://www.bio-logic.fr/rapid-kinetics/specfit.html) and processed using global analysis methods. Kinetics of dichloramine formation was investigated using excess HOCl (up to 2-fold) over free amine, and absolute rate constants determined from single wavelength fits using Origin 7.0 software (OriginLab, Northampton, MA, U.S.A.). All second-order rate constants are means ± S.D. for $n > 4$ determinations.

Quantification of N-chloro derivatives

TNB (5-thio-2-nitrobenzoic acid; 35–45 μM) was used to quantify the yield of N-chloro derivatives after 15 min incubation at 22 °C using ε_{412} 13 600 $M^{-1} \cdot cm^{-1}$ [23]; 30 min incubations were employed in the case of the polymer-derived chloramines and dichloramines as these species react more slowly with TNB.

Quantification of $GlcNH_2$ residues in glycosaminoglycans

The free amino groups ($R\text{-}NH_2$) of polysaccharide-derived $GlcNH_2$ residues were initially assayed with fluorescamine reagent [24] using glucosamine hydrochloride as a standard. The abundances of $GlcNH_2$ residues in p-HS and dnsp-HP determined by this method were 26 and 103 $\mu mol \cdot mg^{-1}$ respectively (with respect to dry weight). An additional preparation of dnsp-HP was determined to have a $GlcNH_2$ residue content of 142 $\mu mol \cdot mg^{-1}$. However, in subsequent studies on the reactions of HOCl with the $GlcNH_2$-containing polymers (dnsp-HP and p-HS; see the Results section), it became apparent that the true concentrations of polymer-derived free amino groups were higher than those measured by the fluorescamine assay.

Monochloramines were detected in high yield (by assay with TNB) as the sole products generated (as assessed by UV–visible spectroscopy) upon reaction of p-HS and dnsp-HP with HOCl in concentrations that were up to approx. 1.5 (p-HS) and 2 (dnsp-HP) times higher than the concentration of $GlcNH_2$ residues determined by the fluorescamine assay. From these results it was concluded that the fluorescamine assay underestimates the true concentration of polymer-derived $GlcNH_2$ residues. This may be due to inefficient derivative formation of polymer-derived amino groups or to low fluorescence of the resulting polymer-bound adducts compared with the monosaccharide-bound adducts. The true concentration of polymer-derived $GlcNH_2$ residues on each polymer was taken as the highest concentration of HOCl that yielded monochloramines as the sole product (i.e. with no residual HOCl to generate dichloramines). The revised estimates of the $GlcNH_2$ residue abundance in p-HS and dnsp-HP were 35 and 206 $\mu mol \cdot mg^{-1}$ respectively (with respect to dry weight); an

Table 1 Residue abundance/substitution data for glycosaminoglycans (expressed per 100 disaccharides)

	p-HS*	dnsp-HP*	p-HP†	b-HP†	HA
$GlcNH_2$	1.7	12.5	0	0	0
$GlcNSO_3$	43.4	76.1	88.6	97.7	0
GlcNAc	55.0	11.4	11.4	2.3	100
2-*O*-sulphate	19.9	75.6	75.6	89.3	0
6-*O*-sulphate	21.9	81.5	81.5	92.4	0
Average molecular mass of disaccharide (Da)‡	470	607	615	645	401

* Data from [25], except for abundance of $GlcNH_2$, which was determined as described in the text; an additional preparation of dnsp-HP used was determined to have the following glycosamine residue abundances (residues per 100 disaccharides): $GlcNH_2$, 17.1; $GlcNSO_3$, 71.5; and GlcNAc, 11.4 (average molecular mass of disaccharide 604 Da).

† Data from [25].

‡ Calculated with respect to dry weight on the basis of the abundance/substitution data; carboxylate and sulphate groups were assumed to have sodium (Na^+) counter-ions, and free amine groups were assumed to exist as hydrochloride (HCl) salts.

additional preparation of dnsp-HP was determined to have a $GlcNH_2$ residue content of 283 μmol · mg^{-1}.

These data, in combination with existing residue abundance/substitution data [25], were used to calculate the average molecular mass of disaccharide repeat units and the abundance of $GlcNH_2$ residues per disaccharide for these polymers (Table 1). With p-HS, the abundance of $GlcNH_2$ residues determined here (Table 1) is within the range of existing data for this polymer (0.7–2.8 % of disaccharides) [26,27].

PAGE

Polymer samples were analysed using 20 % (w/v) polyacrylamide gels (0.1 cm × 16 cm × 20 cm, Protean® II xi system, Bio-Rad Laboratories). Aliquots (40 μl) from reaction mixtures were treated with 5 μl of 200 mM methionine at room temperature (22 °C) for 30 min to quench residual N-chloro compounds, and then stored at − 18 °C before analysis. The 10 × TBE buffer (1 M Tris/0.25 M borate/0.01 M EDTA buffer, pH 8.3) containing 10 μl of 2 M sucrose was added to 45 μl of sample; 25–50 μl of these solutions (approx. 116 μg of polymer) were loaded on to 20 % polyacrylamide gels. Heparin octasaccharides (10 μg) were loaded in a similar manner. Gels were run at 75 V for 15 h at room temperature with 1 × TBE used as running buffer and were subsequently stained with 0.5 % Alcian Blue in 2 % (v/v) acetic acid and destained with 2 % acetic acid. Gel images were acquired using a Umax PowerLook 1120 flatbed scanner and Silverfast Ai 6.0 software (Umax Technologies, Dallas, TX, U.S.A.) or using a Bio-Rad Gel Doc 2000 system and Bio-Rad Quantity One software (Bio-Rad). Gel images were digitized over a linear range using Bio-Rad Quantity One software (Bio-Rad).

Computational modelling of HOCl reactivity with isolated glycosaminoglycans and proteoglycans

The modelling of the reactivity of HOCl with the isolated glycosaminoglycans and proteoglycans was performed with Specfit software. For each species examined, the computational model consisted of a series of individual reactions describing its full reactivity together with abundance data. The software was allowed to undergo 100 iterations to yield predicted reactant and product concentrations at time intervals that corresponded to experimental methods (isolated glycosaminoglycans) or with complete consumption of HOCl (proteoglycans).

Modelling of the reaction of HOCl with isolated glycosaminoglycans was performed using abundance data given in Table 1 and the second-order rate constants (for reaction with polymer-derived glycosamine residues at 22 or 37 °C as specified) given in Table 2. Modelling of the reaction of HOCl with the heparan sulphate proteoglycans glypican-1 and perlecan was performed using abundance data and second-order rate constants given in Supplementary Table 1 at http://www.BiochemJ.org/bj/391/bj3910125add.htm. The number of reactive side-chain residues and backbone amides present in the core proteins of the proteoglycans were determined from SwissProt (human glypican-1, primary accession number P35052; human perlecan, primary accession number P98160). The abundance of disulphide bonds in glypican-1 has not been reported but it has been assumed for our modelling studies that the 14 invariant cysteine residues among the glypican family [28] are involved in disulphide bonding. With perlecan, at least 104 cysteine residues are predicted to be present as cystines, based on sequence homology to proteins with known composition (data from SwissProt). The proteoglycans have been assumed to be fully substituted with heparan sulphate (perlecan, three chains [29]; and glypican-1, three chains [30]). Each heparan sulphate chain was assumed to have the composition of heparan sulphate isolated from human aorta (molecular mass 45 kDa; four $GlcNH_2$ residues per chain; 39 $GlcNSO_3$ residues per 100 disaccharides; remainder GlcNAc residues [26,31]); human perlecan and glypican-1 are abundant vascular proteoglycans [32] and are probable sources of this material. The second-order rate constants used for the modelling the reaction with the protein core are those reported previously for model peptides [17] with the rate constant for reaction with backbone amides being 0.11 $M^{-1} \cdot s^{-1}$ at 22 °C (data for *N*-acetyl-$(Ala)_3$-OMe [17]). For consistency with the protein data, the second-order rate constants used for modelling the reaction using the glycosaminoglycan components are those for the monosaccharides in Table 2.

Table 2 Second-order rate constants (± S.D., $n \geqslant 4$) for the reaction of HOCl with glycosamine monosaccharides and polymer-derived glycosamine residues at pH 7.4, and structural assignment of product chromophores

Substrate	k_2 (37 °C) ($M^{-1} \cdot s^{-1}$)	Product λ_{max} (nm)	Assigned structure of product
$GlcNH_2$	1.76×10^6*	258	Chloramine (R-NCl-H)
$GlcNH_2$ chloramine	~33†	~300	Dichloramine ($R\text{-}NCl_2$)
$GlcNSO_3$	0.91 ± 0.13‡	272	N-chlorosulphonamide ($R\text{-}NCl\text{-}SO_3^-$)
GlcNAc	0.064 ± 0.003§	< 220	Chloramide ($R\text{-}NCl\text{-}C(O)CH_3$)
Polymer-derived $GlcNH_2$	3.1×10^5‖	254	Chloramine (R-NCl-H)
Polymer-derived $GlcNH_2$ chloramine	~9¶	318	Dichloramine ($R\text{-}NCl_2$)
Polymer-derived $GlcNSO_3$	0.051 ± 0.02	272	N-chlorosulphonamide ($NCl\text{-}SO_3^-$)
Polymer-derived GlcNAc	0.012 ± 0.03	< 220	Chloramide ($R\text{-}NCl\text{-}C(O)CH_3$)

* Estimated from k_2 (9.5 °C) = (3.5 ± 0.1) × 10^5 · $M^{-1} \cdot s^{-1}$ (see text); k_2 (22 °C, estimate) = 7.6 × 10^5 · $M^{-1} \cdot s^{-1}$.

† Estimated from k_2 (22 °C) ~ 14 $M^{-1} \cdot s^{-1}$ (see text).

‡ k_2 (22 °C) = 0.062 ± 0.01 $M^{-1} \cdot s^{-1}$.

§ k_2 (22 °C) = 0.0108 ± 0.0002 $M^{-1} \cdot s^{-1}$.

‖ Estimated from k_2 (10 °C) = (6.4 ± 0.1) × 10^4 $M^{-1} \cdot s^{-1}$ (see text).

¶ Estimated from k_2 (22 °C) ~ 4 $M^{-1} \cdot s^{-1}$ (see text).

RESULTS

Rate constants for reaction of HOCl with glycosamine monosaccharides

Reaction of HOCl (1 mM) with GlcNAc (5–40 mM) at either 22 or 37 °C resulted in loss of the absorption band of ^-OCl (λ_{max} 292 nm) and concomitant formation of a peak with λ_{max} < 220 nm, with an

isosbestic point observed at 262 nm (Supplementary Figure 1A at http://www.BiochemJ.org/bj/391/bj3910125add.htm). The formation of this new absorption is assigned, as previously, to the GlcNAc chloramide (R-NCl-C(O)CH_3) [20,22]. The kinetic traces fitted well to pseudo-first-order kinetics, and global analysis of these data yielded the second-order rate constant given in Table 2.

Analogous studies with $GlcNSO_3$ (5–40 mM; 1 mM HOCl) at 22 or 37 °C resulted in loss of the $^-$OCl peak and concomitant formation of a peak with λ_{max} 272 nm and increased absorbance in the low-UV region; isosbestic points were observed at 228, 244 and 270 nm (Supplementary Figure 1C at http://www.BiochemJ.org/bj/391/bj3910125add.htm). Global analysis of these data yielded the second-order rate constant given in Table 2. The peak with λ_{max} 272 nm and the increased absorbance in the low-UV region are assigned to the $GlcNSO_3$ N-chlorosulphonamide (R-NCl-SO_3^-).

With $GlcNH_2$ (1–5 mM; 1 mM HOCl) under analogous conditions, a rapid loss of the $^-$OCl peak (within 30 s) and formation of a peak with λ_{max} 258 nm (Supplementary Figure 1E, inset, at http://www.BiochemJ.org/bj/391/bj3910125add.htm) were detected. This λ_{max} value is characteristic of monochloramines [23], and is assigned to the $GlcNH_2$ monochloramine (R-NCl-H). As the kinetic data obtained were limited by the dead time of the stopped-flow system at these temperatures, experiments were carried out at 9.5 °C to slow the reaction down. Global analysis of data obtained under these conditions with $GlcNH_2$ (0.25–1.0 mM) and HOCl (0.1–0.2 mM) (Supplementary Figure 1E at http://www.BiochemJ.org/bj/391/bj3910125add.htm) yielded a second-order rate constant for this reaction at 9.5 °C (Table 2). Rate constants for reaction at 22 and 37 °C (Table 2) were estimated using the Arrhenius equation with an activation energy (E_a) of 43 kJ · mol^{-1}; the latter value is the experimentally determined E_a for the reaction of HOCl with 2-propylamine [33], a close structural analogue of the $GlcNH_2$-derived amine function.

As monochloramines of primary amines (R-NCl-H) can react further with HOCl to yield dichloramines (R-NCl_2), the formation of such species was also investigated. Dichloramines have a characteristic absorbance peak with λ_{max} approx. 300–310 nm and a shoulder of absorbance at < 250 nm [23].

Reaction of equimolar concentrations of $GlcNH_2$ and HOCl (both 1 mM) at 22 °C, gave solely the $GlcNH_2$ monochloramine (λ_{max} 258 nm; Supplementary Figure 1E at http://www.BiochemJ.org/bj/391/bj3910125add.htm), which was stable for 45 min under these conditions. In contrast, reaction of $GlcNH_2$ (1 mM) with excess HOCl (1.1–2.5 mM) yielded spectra that underwent two distinct phases of absorbance decay that were complete within 45 min under all reaction conditions (Supplementary Figure 1G at http://www.BiochemJ.org/bj/391/bj3910125add.htm). During the first phase of decay, absorbance at approx. 258 nm (monochloramine) and approx. 292 nm ($^-$OCl) decreased in tandem, consistent with reaction of the initially formed monochloramine with HOCl to form a dichloramine. With higher excesses of HOCl (HOCl/$GlcNH_2 > 2$), formation of a peak at > 292 nm was apparent during the first phase of decay, consistent with the presence of the dichloramine (Supplementary Figure 1G at http://www.BiochemJ.org/bj/391/bj3910125add.htm). During the second phase of decay, absorbance in the low-UV region (< 250 nm) and at > 292 nm decreased in tandem, consistent with dichloramine decomposition (Supplementary Figure 1G at http://www.BiochemJ.org/bj/391/bj3910125add.htm). After these two phases of decay were completed, a residual monochloramine peak was detected with HOCl/$GlcNH_2$ ratios in the range 1–2 (results not shown) but this species was absent for higher excesses of HOCl.

Overall, these results are consistent with rapid quantitative conversion of $GlcNH_2$ into the monochloramine, and further reaction of this species with excess HOCl to give an unstable dichloramine. While the absorbance changes in these experiments are complex and cannot be fitted exactly at all wavelengths by global analysis methods, the consumption of monochloramine (at 258 nm) by excess HOCl (with HOCl/$GlcNH_2$ ratios in the range 1–2) was readily fitted with a single exponential, providing an estimate of the second-order rate constant for formation of the dichloramine from the monochloramine (Table 2). At 37 °C, direct determination of this rate constant was not possible due to rapid dichloramine decomposition; this rate constant was estimated as for monochloramine formation (see above), assuming the same activation energy.

Rate constants for reaction of HOCl with the glycosamine residues of heparin and heparan sulphate

The quantitative importance of the reaction at each of the glycosamine residues present in heparan sulphate and heparin will be determined by both the reactivity and the abundance of these residues. Abundance data for glycosamine residues in heparin and heparan sulphate have been reported previously [25–27]; these data vary little for material isolated from a given biological source and tissue. Previous data for the polymers [25], and for $GlcNH_2$ residues determined in the present study (see the Experimental section), are summarized in Table 1.

Kinetics of polymer-derived chloramide formation

The rate constant for reaction of HOCl with polymer-derived GlcNAc residues was determined using HA, as GlcNAc residues are the only glycosamine residues present in this polymer (Table 1). Reaction of HOCl (1 mM) with HA (4.01–16.04 mg · ml^{-1}; 10–40 mM GlcNAc residues) resulted in loss of the $^-$OCl peak and concomitant formation of a peak with $\lambda_{max} < 220$ nm that is assigned to chloramides (cf. the monosaccharide data; Supplementary Figure 1B at http://www.BiochemJ.org/bj/391/bj3910125add.htm) consistent with previous results [22]. Global analysis of these data yielded the second-order rate constant given in Table 2.

Kinetics of polymer-derived N-chlorosulphonamide formation

The rate of reaction of HOCl with polymer-derived $GlcNSO_3$ residues was investigated using heparin, as $GlcNSO_3$ residues are the predominant glycosamine in this polymer (Table 1). Reaction of HOCl (1–5 mM) with p-HP (1.6–12.8 mg · ml^{-1}; 2.6–19.8 mM $GlcNSO_3$ residues) or b-HP (6.4 mg · ml^{-1}; 9.9 mM $GlcNSO_3$ residues) resulted in the loss of the $^-$OCl peak and concomitant formation of a peak with λ_{max} 272 nm and increasing absorbance in the short wavelength UV region (Supplementary Figure 1D at http://www.BiochemJ.org/bj/391/bj3910125add.htm). The peak with λ_{max} 272 nm is assigned to N-chlorosulphonamides (cf. monosaccharide data). The kinetic data obtained with p-HP fitted well by global analysis using a reaction model involving attack solely at $GlcNSO_3$ residues; the derived second-order rate constant is given in Table 2. The greater reactivity of polymer-derived $GlcNSO_3$ towards HOCl, compared with GlcNAc residues (cf. HA data), is in accordance with the monosaccharide data (Table 2).

Kinetics of polymer-derived mono- and dichloramine formation

In contrast with native heparin, p-HS and its structural analogue dnsp-HP contain $GlcNH_2$ residues in addition to $GlcNSO_3$

and GlcNAc (Table 1). Reaction with HOCl would therefore be expected to yield polymer $GlcNH_2$-derived mono- and di-chloramines, in addition to N-chlorosulphonamides and chloramides.

Formation of polymer-derived monochloramines was investigated initially at 22 °C using p-HS and dnsp-HP. Reaction of the polymers (6.4 mg · ml^{-1} each) with HOCl ($\leqslant$ 0.45 mM with p-HS; $\leqslant$ 1.32 mM or $\leqslant$ 1.82 mM with the two preparations of dnsp-HP) under these conditions resulted in rapid decay of the $^{-}$OCl peak (< 0.5 s) and an accompanying increase in absorbance at shorter wavelengths. Difference spectra, obtained by subtraction of the absorbance of the unchanged parent polymer, showed the presence of a peak with λ_{max} 254 nm (Supplementary Figure 1F, inset, at http://www.BiochemJ.org/bj/391/bj3910125add.htm). This absorbance is assigned to polymer-derived monochloramines on the basis of its characteristic λ_{max} value [23], and the data obtained with the monosaccharide analogue (Table 2 and Supplementary Figure 1E at http://www.BiochemJ.org/bj/391/bj3910125add.htm).

Evidence for the formation of polymer-derived dichloramines was obtained with higher concentrations of HOCl (> 0.45 mM with p-HS; > 1.32 mM or > 1.82 mM with the two preparations of dnsp-HP) at 22 and 37 °C. Thus with dnsp-HP (Supplementary Figure 1H at http://www.BiochemJ.org/bj/391/bj3910125add.htm), absorbance changes were detected that were consistent with consumption of initially formed monochloramines (λ_{max} 254 nm) by residual HOCl ($^{-}$OCl λ_{max} 292 nm) to give a species which has an absorbance band in the low-UV region (< 250 nm) and a peak with λ_{max} 318 nm (obtained from difference spectra as outlined above; Supplementary Figure 1H, inset, at http://www.BiochemJ.org/bj/391/bj3910125add.htm). These absorbance bands are assigned to polymer-derived dichloramines by comparison with previous data [23,34]. In analogous studies with p-HS, similar absorbance changes were detected, consistent with rapid monochloramine formation, followed by slower dichloramine formation. In this case, the dichloramine peak was not observed due to the low absorbance of the N-chloro species relative to the background absorbance of the polymer.

The rate constant for formation of polymer-derived monochloramines was estimated using data obtained at 9.5 °C with ratios of HOCl/$GlcNH_2$ residues < 1. Global analysis of the data obtained with dnsp-HP (4.8–9.6 mg · ml^{-1}; 0.99–1.98 mM $GlcNH_2$ residues) and HOCl (100–200 μM; Supplementary Figure 1F at http://www.BiochemJ.org/bj/391/bj3910125add.htm) yielded a second-order rate constant for polymer-derived monochloramine formation (Table 2). The absorbance changes detected at higher temperature (22 and 37 °C) were too fast to obtain accurate second-order rate constants; the rate constants at these temperatures (Table 2) were estimated using the data obtained at 9.5 °C, as described for the corresponding monosaccharide-derived monochloramine.

The rate constant for formation of polymer-derived dichloramines was estimated using data obtained at 22 °C using conditions where the ratio of HOCl/$GlcNH_2$ was in the range 1–2. With dnsp-HP (6.4 mg · ml^{-1}; 1.32 mM $GlcNH_2$ residues) and HOCl (1.65–1.98 mM), single exponential fits to the time-dependent data at 230, 254 and 330 nm, where the chloramine and dichloramine absorb, yielded a second-order rate constant for this reaction (Table 2). This analysis assumes quantitative conversion of polymer $GlcNH_2$ residues into chloramines, followed by reaction of excess HOCl with the chloramines on a timescale that is independent of chloramine formation. The rate constant for the formation of polymer-derived dichloramines at 37 °C (Table 2) was estimated using the data obtained at 22 °C, as described for the corresponding monosaccharide-derived dichloramine.

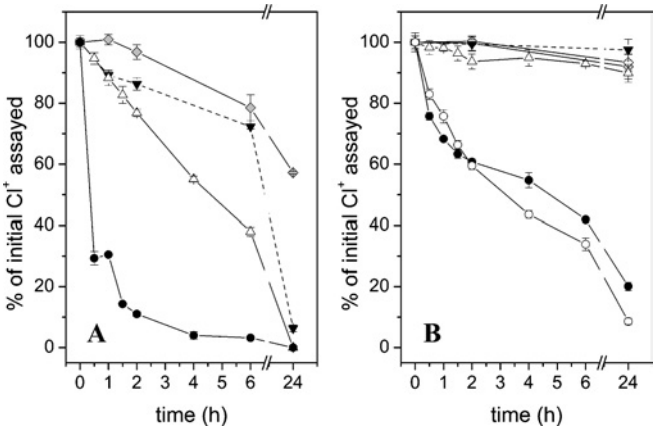

Figure 2 Stability of N-chloro derivatives of glycosaminoglycans and glycosamine monosaccharides on incubation at 37 °C in pH 7.4 buffer

Time-dependent changes in the concentrations of N-chloro derivatives were determined by assay with TNB and expressed as percentage of the initial value. Monosaccharide and polymer N-chloro derivatives were prepared as described in the text. The preparation of polymer dichloramines was initially assayed 0.5 min after the addition of HOCl, i.e. before complete HOCl consumption (see text). Data for HA chloramides is reproduced from [22]. (**A**) Monosaccharide N-chloro derivatives: $GlcNH_2$ dichloramines (●); $GlcNH_2$ chloramines (△); $GlcNSO_3$ N-chlorosulphonamides (grey diamonds); GlcNAc chloramides (▼). (**B**) Polymer N-chloro derivatives: p-HS dichloramines (●), dnsp-HP dichloramines (○), dnsp-HP chloramines (△), p-HP NCl (grey diamonds), b-HP NCl (◇) and HA chloramides (▼).

Quantification and stability of the N-chloro derivatives of heparin and heparan sulphate and their constituent glycosamine monosaccharides

Stability of N-chlorinated monosaccharides

The $GlcNSO_3$ N-chlorosulphonamide and the GlcNAc chloramide were prepared by reaction of HOCl (0.45 mM) with the parent monosaccharides ($GlcNSO_3$, 37 °C, 15 min; GlcNAc, 37 °C, 90 min) in yields of 78 and 88 % with respect to added HOCl. Further incubation of these species at 37 °C resulted in approx. 20–25 % loss within 6 h; chloramide decomposition was complete after 24 h but approx. 60 % of the N-chlorosulphonamide remained (Figure 2A).

The $GlcNH_2$ monochloramine was prepared in approx. 100 % yield, with respect to added HOCl, by reaction of equimolar $GlcNH_2$ and HOCl (1 mM each) at 22 °C for 30 s. Subsequent incubation at 37 °C resulted in approx. 60 % decomposition within 6 h and complete decomposition within 24 h (Figure 2A). The corresponding dichloramine was prepared by reaction of $GlcNH_2$ (1 mM) with HOCl (2 mM) at 22 °C for 5 min. At this time point, the dichloramine was detected in approx. 50 % yield with respect to added HOCl. After 30 min incubation at 37 °C, 70 % of the N-chloro species had decomposed (Figure 2A). These data are consistent with rapid formation and decomposition of the $GlcNH_2$ dichloramine to yield non-TNB-reactive species; this rapid decomposition is in accordance with the data obtained by UV–visible spectroscopy.

Stability of N-chlorinated polymers

N-chloro derivatives of b-HP and p-HP were prepared by reaction of the parent polymers (6.4 mg · ml^{-1}; 9.9 and 10.4 mM in disaccharides respectively) with excess HOCl (40.9 mM) at 37 °C for 16 min with subsequent removal of residual HOCl by size-exclusion (PD10) chromatography; this yielded 2.5–2.7 mM N-chloro species as assayed by TNB. These preparations are henceforth referred to as b-HP NCl and p-HP NCl.

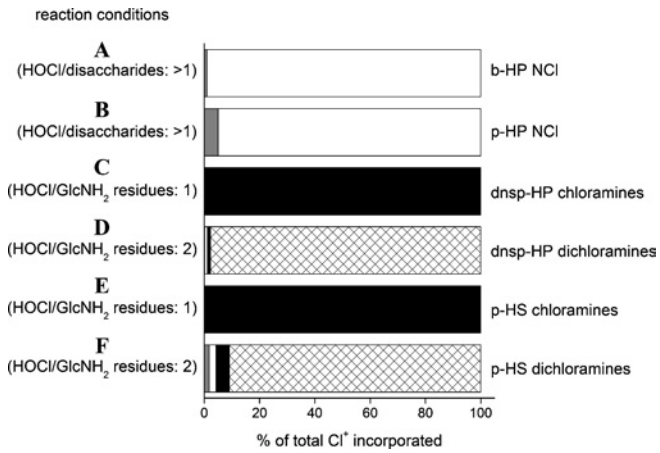

Figure 3 Computational modelling of the preparation of glycosaminoglycan N-chloro derivatives at 22 or 37 °C and pH 7.4

Predicted yields of polymer-derived N-chloro derivatives, expressed as percentage of total chlorine (Cl^+) incorporated. $GlcNH_2$-derived chloramines (R-NCl-H; black bars), $GlcNH_2$-derived dichloramines ($R\text{-}NCl_2$; cross-hatched bars), $GlcNSO_3$-derived N-chlorosulphonamides ($R\text{-}NCl\text{-}SO_3^-$; white bars) and GlcNAc-derived chloramides ($R\text{-}NCl\text{-}C(O)CH_3$; grey bars). Yields were predicted with Specfit software using computational reaction models that incorporate data for the abundance of glycosamine residues in the various polymers (Table 1) and the rate constants for reaction at these residues (Table 2). The following reaction conditions were modelled. (**A**) b-HP (6.4 mg · ml^{-1}; 9.67 mM $GlcNSO_3$, 0.23 mM GlcNAc) reacted with HOCl (40.9 mM) at 37 °C for 16 min. (**B**) As in (**A**) except with p-HP (6.4 mg · ml^{-1}; 9.22 mM $GlcNSO_3$, 1.19 mM GlcNAc). (**C**) dnsp-HP (6.4 mg · ml^{-1}; 1.815 mM $GlcNH_2$, 7.58 mM $GlcNSO_3$, 1.21 mM GlcNAc) reacted with HOCl (1.815 mM) at 22 °C for 30 s. (**D**) As in (**C**) except with HOCl (3.63 mM) at 37 °C for 30 min. (**E**) p-HS (6.4 mg · ml^{-1}; 0.225 mM $GlcNH_2$, 5.90 mM $GlcNSO_3$, 7.47 mM GlcNAc) reacted with HOCl (0.225 mM) at 22 °C for 30 s. (**F**) As in (**E**) except with HOCl (0.45 mM) at 37 °C for 30 min.

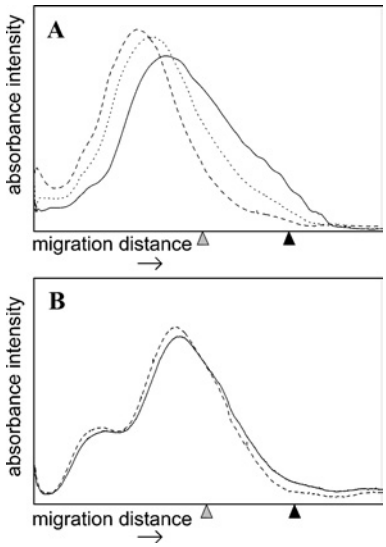

Figure 4 Dichloramine-dependent fragmentation of glycosaminoglycans at 37 °C and pH 7.4

Densitometric traces of polymer samples analysed by PAGE with Alcian Blue staining. (**A**) dnsp-HP (6.4 mg · ml^{-1}; 1.815 mM $GlcNH_2$ residues) reacted with HOCl (3.63 mM) at 37 °C for 0 (– – –), 6 (· · · ·), and 24 h (———). (**B**) p-HS (6.4 mg · ml^{-1}; 0.225 mM $GlcNH_2$ residues) reacted with HOCl (0.45 mM) at 37 °C for 0 (– – –) and 24 h (———). Grey arrowhead, migration position of Bromophenol Blue; black arrowhead, migration position of heparin octasaccharide standards.

Computational modelling using the kinetic and composition data (Tables 2 and 1 respectively) predicts that N-chlorosulphonamides are the predominant species formed under these conditions (Figure 3). Both b-HP NCl and p-HP NCl showed minimal decomposition upon incubation at 37 °C for 24 h ($\lesssim$ 10 % loss of N-chloro species; Figure 2B). Thus polymer-derived N-chlorosulphonamides have similar stability to polymer-derived chloramides (e.g. those generated on HA [22]) (Figure 2B).

Upon reaction of dnsp-HP and p-HS (6.4 mg · ml^{-1}; 0.45–1.82 mM $GlcNH_2$ residues) with HOCl (0.45–1.82 mM; HOCl/$GlcNH_2 = 1$) at 22 °C for 30 s, N-chloro species were detected in yields of 81–83 % with respect to added HOCl. These N-chloro species are predicted to consist almost exclusively of monochloramines by computational modelling (Figure 3) and are henceforth referred to as dnsp-HP chloramines and p-HS chloramines. Over 24 h at 37 °C, the loss of N-chloro species was 10 and 51 % for dnsp-HP chloramines and p-HS chloramines respectively (Figure 2B).

Upon reaction of dnsp-HP and p-HS with a 2-fold excess of HOCl over $GlcNH_2$ residues (6.4 mg · ml^{-1} polymer, 0.9–3.63 mM HOCl) at 37 °C, the total chlorine (Cl^+, i.e. N-chloro species and residual HOCl) detected after 30 s was 71–75 % with respect to added HOCl. On further incubation at 37 °C for 30 min, the measured yields of N-chloro species were 76–83 % of the initial Cl^+ assayed (Figure 2B). HOCl consumption is predicted to be complete at this time point with dichloramines being the major N-chloro species generated (Figure 3). The losses in Cl^+ preceding this time point are attributed to the formation and decomposition of polymer-derived dichloramines. After 6 and 24 h incubation, only 58–66 % and 80–91 % respectively of the initial Cl^+ remained (Figure 2). The rate and extent of dichloramine decomposition detected under these conditions matches with the UV–visible spectroscopic data (Supplementary Figure 1H, inset, at http://www.BiochemJ.org/bj/391/bj3910125add.htm).

Effect of the formation of N-chloro derivatives on the structural integrity of heparin and heparan sulphate

Changes in the molecular mass of the polymers after N-chlorination, and subsequent incubation at 37 °C for 24 h, was assessed by PAGE with Alcian Blue staining [35]. No detectable changes in molecular mass occurred as a consequence of the formation and subsequent incubation of N-chlorosulphonamides on b-HP and p-HP, nor of monochloramines formed on p-HS and dnsp-HP (results not shown), consistent with the slow decomposition of these N-chloro derivatives under these conditions (cf. Figure 2B). In contrast, the formation and subsequent decomposition of dnsp-HP dichloramines and p-HS dichloramines was accompanied by significant decreases in average molecular mass, which is attributed to fragmentation of the polymer backbone (Figure 4). With dnsp-HP dichloramines, the time course of fragmentation paralleled the time course of dichloramine decomposition detected by assay with TNB (cf. Figure 2B) and UV–visible absorption (see Supplementary Figure 1H, inset, at http://www.BiochemJ.org/bj/391/bj3910125add.htm), although with a slight lag. Thus whilst the majority of the dichloramines had decomposed after 6 h, the majority of fragmentation occurred after this time point (Figure 4). These data suggest that fragmentation is a consequence of dichloramine decomposition. The relatively small decrease in average molecular mass (i.e. fragmentation) detected on decomposition of p-HS dichloramines is attributed to cleavage near the termini of the polymer chains, where the $GlcNH_2$ residues are located in this polymer [26], and the low abundance of these sites of cleavage ($\sim$0.5 per polymer chain). Similarly small changes in molecular mass (as assessed by gel chromatography) have been observed previously upon chemical cleavage of p-HS at $GlcNH_2$ residues with nitrous acid [26].

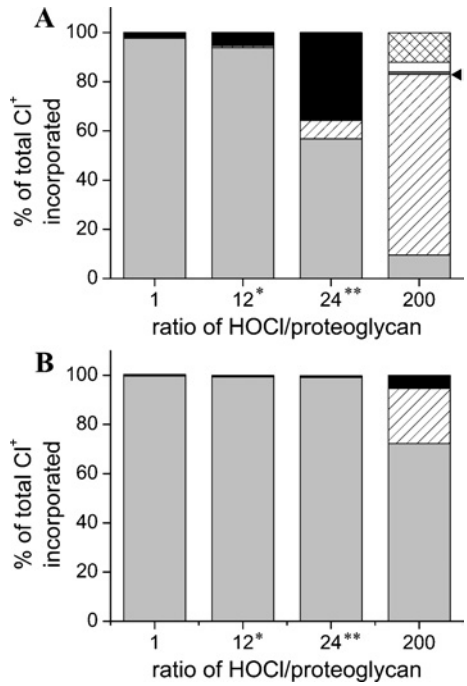

Figure 5 Computational modelling of the reaction of HOCl with the protein core and glycosaminoglycan chains of proteoglycans at 22 °C and pH 7.4

Predicted consumption of HOCl by proteoglycan protein core and attached glycosaminoglycan chains expressed as percentage of total chlorine (Cl^+) incorporated. (**A**) Human glypican-1. (**B**) Human perlecan. Black bars, heparan sulphate-derived $GlcNH_2$ (to give chloramines); cross-hatched bars, heparan sulphate-derived $GlcNH_2$ (to give dichloroamines); white bars, heparan sulphate-derived $GlcNSO_3$ (to give N-chlorosulphonamides), dark grey bars, heparan sulphate-derived GlcNAc (to give chloramides), indicated by arrowhead; light grey bars, protein residues (total of cysteine, cystine and methionine side chains); hatched bars, total of remaining protein components; *, HOCl/$GlcNH_2$ residues ratio of 1; **, HOCl/$GlcNH_2$ residues ratio of 2.

Computational modelling of the extent of reaction of HOCl with the protein and glycosaminoglycan components of proteoglycans

By combining the rate constants determined in the present study with those obtained previously for the protected amino acids and model compounds [17] the reactivity of HOCl with proteoglycans of known composition can be predicted. These species are likely to be major targets for HOCl, as MPO is released extracellularly, and is known to bind electrostatically with proteoglycans as a result of the polyanionic nature of the glycosaminoglycan chains and the cationic nature of MPO [2,7,8].

The predicted partitioning between the protein and carbohydrate sites of glypican-1 (a glycosylphosphatidylinositol-anchored cell-surface proteoglycan) and perlecan (a secreted proteoglycan) treated with various excesses of HOCl are given in Figure 5. With both proteoglycans, protein cysteine and methionine residues are consumed first, due to their high reactivity, with reaction at these sites accounting for almost all of the HOCl added at a HOCl/proteoglycan molar ratio $\leqslant 1$. However, with higher excesses of HOCl, the predicted distribution of attack differs considerably between the two proteoglycans, due to differences in the core protein structures. Glypican-1 contains a small protein core with relatively few cysteine and methionine residues, whereas perlecan has a large, multidomain protein core with an abundance of cysteine and methionine residues (see Supplementary Table 1 at http://www.BiochemJ.org/bj/391/bj3910125add.htm).

With glypican-1, the $GlcNH_2$ residues of the heparan sulphate chains represent a significant target at HOCl/proteoglycan molar ratios >1. When HOCl is present in a 2-fold molar excess over the $GlcNH_2$ residues of glypican-1 (24-fold overall molar excess of HOCl; Figure 5A), these residues are major sites of reaction. Under these conditions, the cysteine and methionine residues are completely oxidized and residual HOCl is consumed mainly by $GlcNH_2$ residues to form monochloramines. At higher excesses of HOCl (HOCl/proteoglycan ratio of 200), significant formation of $GlcNH_2$-derived dichloramines is predicted along with N-chlorosulphonamides and chloramides. Protein backbone chloramides are also major products under these conditions.

With perlecan, reaction at cysteine and methionine residues accounts for most of the HOCl consumed over a wide range of HOCl excesses, even when HOCl is present in a 2-fold molar excess over the $GlcNH_2$ residues (24-fold overall excess; Figure 5B). At higher excesses of HOCl (HOCl/proteoglycan ratio of 200), cysteine and methionine residues are consumed completely and the remaining HOCl reacts with heparan sulphate $GlcNH_2$ residues to give $GlcNH_2$-derived monochloramines, as well as at other sites on the protein core (Figure 5B).

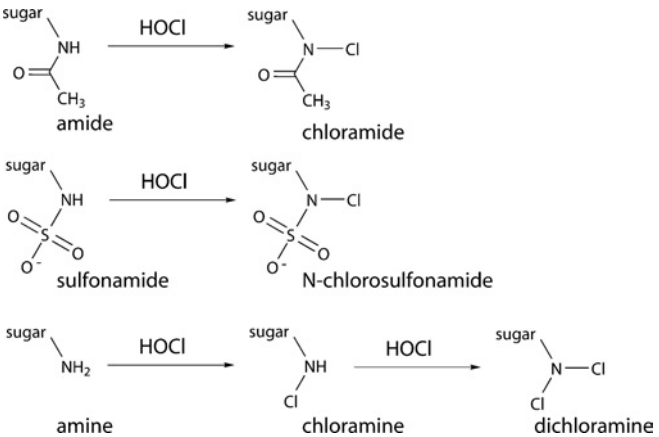

Scheme 1 Formation of N-chloro derivatives on reaction of HOCl with glycosamine-derived amides, sulphonamides and amines

DISCUSSION

In the present study, it has been shown that the MPO-derived oxidant HOCl reacts selectively with the glycosamine residues of heparan sulphate and heparin via N-chlorination (Scheme 1) as assessed by both UV–visible spectroscopy and quantification of the resulting N-chloro derivatives with TNB. Analysis of time-dependent UV–visible spectroscopic data by global analysis techniques has provided, for the first time, second-order rate constants for reaction of HOCl at each type of glycosamine residue. Evidence has been obtained for very rapid reaction of HOCl with polymer-derived $GlcNH_2$ residues to form monochloramines (R-NCl-H) ($k_2 \sim 3.1 \times 10^5\ M^{-1} \cdot s^{-1}$ at 37 °C) and for subsequent reaction of these species to generate dichloramines ($R\text{-}NCl_2$) ($k_2 \sim 9\ M^{-1} \cdot s^{-1}$ at 37 °C). Slower reactions occur with polymer-derived $GlcNSO_3$ residues to generate N-chlorosulphonamides ($R\text{-}NCl\text{-}SO_3^-$) ($k_2 \sim 0.051\ M^{-1} \cdot s^{-1}$ at 37 °C) and GlcNAc residues to generate chloramides ($R\text{-}NCl\text{-}C(O)CH_3$) ($k_2 \sim 0.012\ M^{-1} \cdot s^{-1}$ at 37 °C). These polymer rate constants are lower than those for reaction of HOCl with the corresponding monosaccharides, possibly due to steric crowding and charge effects; this is consistent with previous data [22].

The high rate constants determined for reaction with $GlcNH_2$ show that these residues are a major target for HOCl. These values are approx. 70-fold higher than those for the reaction of HOCl

with the side-chain amine group of lysine residues ($k_2 \sim 3.5 \times 10^5\ M^{-1} \cdot s^{-1}$ for $GlcNH_2$ monosaccharide at 9.5 °C versus $5 \times 10^3\ M^{-1} \cdot s^{-1}$ for N-acetyl-lysine at 10 °C [17]), and are also markedly greater than for reaction of HOCl with N-terminal NH_2 groups of free amino acids ($k_2 \sim 0.3–1 \times 10^5\ M^{-1} \cdot s^{-1}$ at 10 °C [17]). These rate constants are also greater than those reported for a wide range of other amino acid side chains (or appropriate models) including disulphide bonds, histidine, tryptophan, tyrosine, phenylalanine and arginine residues and backbone amide sites [17]), but smaller than those for the two most reactive side chains on proteins – cysteine and methionine residues ($k_2 \sim 3 \times 10^7$ and $4 \times 10^7\ M^{-1} \cdot s^{-1}$ respectively) [17]. The rate constant for subsequent reaction of $GlcNH_2$-derived monochloramines to form dichloramines ($k_2 \sim 14\ M^{-1} \cdot s^{-1}$ at 22 °C for monosaccharide $GlcNH_2$ chloramine) is similar to that previously reported for reaction of tyrosine to form 3-chloro-Tyr ($k_2 \sim 44\ M^{-1} \cdot s^{-1}$ for the phenol side chain of tyrosine residue at 22 °C [17]). This suggests that dichloramine formation on $GlcNH_2$ residues is likely to occur *in vivo*, as chlorinated tyrosine residues have been detected, for example, in atherosclerotic lesions [36]. The rate constants for the formation of $GlcNH_2$-derived dichloramines, $GlcNSO_3$-derived N-chlorosulphonamides and GlcNAc-derived chloramides are of similar magnitude to those determined for the formation of chloramides from protein backbone amides [17].

The rate constants determined in the present study, together with abundance data for the different residue types in glycosaminoglycans, allow the reactivity of HOCl with isolated glycosaminoglycans to be predicted using a computational model. With existing data for the reaction of HOCl with proteins [17] and appropriate composition data, these data have been used to create computational models that predict the reactivity of HOCl with proteoglycans. As data are available for the reactivity of lipids and antioxidants [16], there is further potential to model the reaction of HOCl with more complex targets.

The computational model predicts that reaction of low levels of HOCl with heparan sulphate (molar ratio of HOCl/$GlcNH_2$ residues $\leqslant 1$) results in exclusive formation of monochloramines due to the extremely high reactivity of the $GlcNH_2$-derived amine function. When the molar ratio of HOCl/$GlcNH_2$ residues is in the range 1–2, monochloramines are generated initially, but these react preferentially with residual HOCl to generate dichloramines. At higher molar ratios of HOCl/$GlcNH_2$ residues (> 2) significant reaction also occurs with $GlcNSO_3$ and GlcNAc residues but formation of N-chlorosulphonamides predominates due to the higher rate constant for reaction with $GlcNSO_3$ residues. In contrast, N-chlorosulphonamides are predicted to be formed almost exclusively with heparin, as $GlcNSO_3$ residues predominate and no $GlcNH_2$ residues are present.

The glycosaminoglycan-derived monochloramines, N-chlorosulphonamides and chloramides are relatively long-lived at physiological pH and temperature in the absence of other added reagents, and their formation does not appear to have major effects on the structural integrity of the polymers under the conditions employed. In contrast, polymer-derived dichloramines have been shown to undergo ready decomposition under these conditions, with this process initiating fragmentation of the polymer backbone. The precise mechanism of such fragmentation is unknown, and is the subject of studies currently under way in our laboratory.

All of the monosaccharide-derived N-chloro species proved to be less stable than the corresponding polymer analogues; this is likely to relate to the presence of reactive (reducing) end-groups on the monosaccharides that may undergo redox reactions with the N-chloro derivatives [37]. Reducing monosaccharides can generate one-electron reductants, such as low-valent metal ions and superoxide radicals, via autoxidation and other reactions [38], which are known to decrease the stability of N-chloro species [20–22]. The formation of such species will occur to a much more limited extent with the polymers due to the lower concentration of reducing end groups. The stability and subsequent reactions of N-chloro derivatives of heparan sulphate and related monosaccharides in the presence of metal ions and superoxide radicals will be reported elsewhere.

Modelling of the reaction of HOCl with the cell-surface proteoglycan glypican-1 and the extracellular matrix proteoglycan perlecan has provided data on the likely distribution of attack between the protein and carbohydrate components. While protein cysteine and methionine residues are targeted preferentially over all other sites, reaction at heparan sulphate $GlcNH_2$ residues to generate mono- and dichloramines is predicted to account for the majority of the remaining HOCl. As these two proteoglycans represent extremes in terms of both size and cysteine/methionine content, it is likely that $GlcNH_2$ residues are significant targets for reaction with HOCl in a variety of biological milieu. With glypican-1 and high excesses of HOCl, significant formation of protein backbone chloramides (which are known to result in protein fragmentation [39,40]) is predicted in addition to glycosaminoglycan-derived dichloramines, N-chlorosulphonamides and chloramides.

Detailed structural analyses of the damage induced by HOCl to specific proteoglycans have yet to be performed, although it is clear that these molecules can be damaged and degraded by an MPO-H_2O_2-Cl^- system, as evidenced by release of ^{35}S-labelled material from endothelial cell matrix heparan sulphate proteoglycan (i.e. perlecan) [41]. The modelling data reported here suggest that damage to both protein and glycosaminoglycan sites occurs, and this is consistent with studies where cell culture-derived extracellular matrix has been treated with HOCl; in these previous studies, N-chloro species were detected, and release of both protein and carbohydrate components of the matrix quantified [8]. The modelling approach is however limited by the fact that it does not incorporate important factors which are likely to affect reactivity; these include the accessibility of components that are buried within the three-dimensional structure, the localized steric and charge environment of protein components, and the influence of the localized production of HOCl by MPO on the selectivity of attack [16,17].

A number of studies have quantified the concentrations of HOCl formed *in vivo* under both physiological and pathological conditions. It has been reported that activation of 5×10^6 neutrophil cells $\cdot$ ml^{-1} (the concentration of circulating neutrophils) generates 300–400 μM HOCl over 1–2 h [42,43], with 2.5–5 mM HOCl produced at sites of inflammation [44]. The concentrations, and molar excesses, employed in the experiments reported here are therefore consistent with those generated *in vivo*, suggesting that chlorination and subsequent fragmentation of heparan sulphate and other glycosaminoglycans may be important processes in inflammatory diseases. There is some experimental evidence that is consistent with this proposal. A loss of heparan sulphate epitopes in glomeruli is associated with pathology in a number of human and experimental proteinuric glomerulopathies [45] and, in the case of human membranous glomerulonephritis, the co-localization of MPO and HOCl-modified proteins in the glomerular basement membrane and podocytes has been demonstrated [10]. Perfusion of MPO and H_2O_2 into the renal arteries of rats has been shown to induce proteinuria [46], although the effect of this treatment on glomerular heparan sulphate is unknown. The antioxidant dimethylthiourea has been shown to protect against loss of glomerular heparan sulphate and proteinuria in

adriamycin nephropathy in rats, with this attributed to scavenging of hydroxyl radicals [47]. Co-localization of MPO and HOCl-modified proteins in the extracellular matrix of human atherosclerotic lesions has been observed [9] and chondroitin sulphate proteoglycans isolated from these sites have been shown to have lower molecular mass than those from healthy tissue [48]. The precise modifications that occur to proteoglycans in atherosclerotic lesions and the processes that give rise to these have yet to be characterized; these are the subjects of studies currently under way in our laboratory.

HOCl-induced modifications to glycosaminoglycans may have a number of important biological consequences. Defined sequences within glycosaminoglycan chains are known to play a key role in regulating the binding of a range of proteins (reviewed in [49]). Formation of N-chloro derivatives would be expected to disrupt such binding, as would polymer fragmentation resulting from the formation and decomposition of $GlcNH_2$-derived dichloramines. For example, HOCl-mediated modification of heparan sulphate $GlcNSO_3$ residues may be of significance as such residues interact with the C-terminal Hep-2 domain of fibronectin resulting in the reorganization of the cellular cytoskeleton and the assembly of focal adhesions [25]. HOCl-mediated modification of heparan sulphate $GlcNH_2$ residues by HOCl may also interfere with glypican recycling as this process involves NO-dependent deaminative cleavage at these sites [50]. Heparan sulphate proteoglycans also impart important physicochemical properties to extracellular matrix [45], and this is likely to be compromised by HOCl-mediated damage. Free heparan sulphate chains have also been shown to possess potent pro-inflammatory properties [14] and fragments generated via oxidative cleavage may promote novel, potentially deleterious cellular behaviour.

We are grateful to the Australian Research Council and the National Health and Medical Research Council for financial support. We also thank Professor P. Lay and Dr A. Levina (School of Chemistry, University of Sydney, Sydney, Australia) for use of the Applied Photophysics stopped-flow system.

REFERENCES

1 Kettle, A. J. and Winterbourn, C. C. (1997) Myeloperoxidase: a key regulator of neutrophil oxidant production. Redox Rep. **3**, 3–15
2 McGowan, S. E. (1990) Mechanisms of extracellular matrix proteoglycan degradation by human neutrophils. Am. J. Respir. Cell Mol. Biol. **2**, 271–279
3 Heinecke, J. W. (1999) Mechanisms of oxidative damage by myeloperoxidase in atherosclerosis and other inflammatory disorders. J. Lab. Clin. Med. **133**, 321–325
4 Stocker, R. and Keaney, Jr, J. F. (2004) Role of oxidative modifications in atherosclerosis. Physiol. Rev. **84**, 1381–1478
5 Malle, E., Buch, T. and Grone, H. J. (2003) Myeloperoxidase in kidney disease. Kidney Int. **64**, 1956–1967
6 Zhang, R., Brennan, M. L., Fu, X., Aviles, R. J., Pearce, G. L., Penn, M. S., Topol, E. J., Sprecher, D. L. and Hazen, S. L. (2001) Association between myeloperoxidase levels and risk of coronary artery disease. JAMA, J. Am. Med. Assoc. **286**, 2136–2142
7 Daphna, E. M., Michaela, S., Eynat, P., Irit, A. and Rimon, S. (1998) Association of myeloperoxidase with heparin: oxidative inactivation of proteins on the surface of endothelial cells by the bound enzyme. Mol. Cell. Biochem. **183**, 55–61
8 Woods, A. A. and Davies, M. J. (2003) Fragmentation of extracellular matrix by hypochlorous acid. Biochem. J. **376**, 219–227
9 Malle, E., Waeg, G., Schrieber, R., Grone, E. F., Sattler, W. and Grone, H. (2000) Immunohistochemical evidence for the myeloperoxidase/H_2O_2/halide system in human atherosclerotic lesions. Eur. J. Biochem. **267**, 4495–4503
10 Grone, H. J., Grone, E. F. and Malle, E. (2002) Immunohistochemical detection of hypochlorite-modified proteins in glomeruli of human membranous glomerulonephritis. Lab. Invest. **82**, 5–14
11 Davies, M. J. and Thomas, A. C. (1985) Plaque fissuring – the cause of acute myocardial infarction, sudden ischaemic death and crescendo angina. Br. Heart J. **53**, 363–373
12 Rops, A. L., van der Vlag, J., Lensen, J. F., Wijnhoven, T. J., van den Heuvel, L. P., van Kuppevelt, T. H. and Berden, J. H. (2004) Heparan sulfate proteoglycans in glomerular inflammation. Kidney Int. **65**, 768–785
13 Noble, P. W. (2002) Hyaluronan and its catabolic products in tissue injury and repair. Matrix Biol. **21**, 25–29
14 Johnson, G. B., Brunn, G. J. and Platt, J. L. (2004) Cutting edge: an endogenous pathway to systemic inflammatory response syndrome (SIRS)-like reactions through toll-like receptor 4. J. Immunol. **172**, 20–24
15 Hawkins, C. L., Pattison, D. I. and Davies, M. J. (2003) Hypochlorite-induced oxidation of amino acids, peptides and proteins. Amino Acids **25**, 259–274
16 Pattison, D. I., Hawkins, C. L. and Davies, M. J. (2003) Hypochlorous acid-mediated oxidation of lipid components and antioxidants present in low-density lipoproteins: absolute rate constants, product analysis and computational modeling. Chem. Res. Toxicol. **116**, 439–449
17 Pattison, D. I. and Davies, M. J. (2001) Absolute rate constants for the reaction of hypochlorous acid with protein side-chains and peptide bonds. Chem. Res. Toxicol. **14**, 1453–1464
18 Armesto, X. L., Canle, M. L., Fernandez, M. I., Garcia, M. V. and Santaballa, J. (2000) First steps in the oxidation of sulfur-containing amino acids by hypohalogenation: very fast generation of intermediate sulfenyl halides and halosulfonium cations. Tetrahedron **56**, 1103–1109
19 Prutz, W. A. (1996) Hypochlorous acid interactions with thiols, nucleotides, DNA, and other biological substrates. Arch. Biochem. Biophys. **332**, 110–120
20 Hawkins, C. L. and Davies, M. J. (1998) Degradation of hyaluronic acid, poly- and monosaccharides, and model compounds by hypochlorite: evidence for radical intermediates and fragmentation. Free Radical Biol. Med. **24**, 1396–1410
21 Rees, M. D., Hawkins, C. L. and Davies, M. J. (2004) Hypochlorite and superoxide radicals can act synergistically to induce fragmentation of hyaluronan and chondroitin sulfates. Biochem. J. **381**, 175–184
22 Rees, M. D., Hawkins, C. L. and Davies, M. J. (2003) Hypochlorite-mediated fragmentation of glycosaminoglycans and related *N*-acetyl glycosamines: evidence for chloramide formation, free radical transfer reactions and site-specific fragmentation. J. Am. Chem. Soc. **125**, 13719–13733
23 Thomas, E. L., Grisham, M. B. and Jefferson, M. M. (1986) Preparation and characterization of chloramines. Methods Enzymol. **132**, 569–585
24 Udenfriend, S., Stein, S., Bohlen, P. and Dairman, W. (1972) Fluorescamine; a reagent for assay of amino acids, peptides, proteins, and primary amines in the picomole range. Science **178**, 871–872
25 Lyon, M., Rushton, G., Askari, J. A., Humphries, M. J. and Gallagher, J. T. (2000) Elucidation of the structural features of heparan sulfate important for interaction with the Hep-2 domain of fibronectin. J. Biol. Chem. **275**, 4599–4606
26 Westling, C. and Lindahl, U. (2002) Location of *N*-unsubstituted glucosamine residues in heparan sulfate. J. Biol. Chem. **277**, 49247–49255
27 Wei, Z., Lyon, M. and Gallagher, J. T. (2005) Distinct substrate specificities of bacterial heparinases against *N*-unsubstituted glucosamine residues in heparan sulfate. J. Biol. Chem. **280**, 15742–15748
28 Fransson, L. A. (2003) Glypicans. Int. J. Biochem. Cell Biol. **35**, 125–129
29 Costell, M., Mann, K., Yamada, Y. and Timpl, R. (1997) Characterization of recombinant perlecan domain I and its substitution by glycosaminoglycans and oligosaccharides. Eur. J. Biochem. **243**, 115–121
30 Mertens, G., VanderSchueren, B., vandenBerghe, H. and David, G. (1996) Heparan sulfate expression in polarized epithelial cells: the apical sorting of glypican (GPI-anchored proteoglycan) is inversely related to its heparan sulfate content. J. Cell Biol. **132**, 487–497
31 Feyzi, E., Saldeen, T., Larsson, E., Lindahl, U. and Salmivirta, M. (1998) Age-dependent modulation of heparan sulfate structure and function. J. Biol. Chem. **273**, 13395–13398
32 Rosenberg, R. D., Shworak, N. W., Liu, J., Schwartz, J. J. and Zhang, L. (1997) Heparan sulfate proteoglycans of the cardiovascular system: specific structures emerge but how is synthesis regulated? J. Clin. Invest. **99**, 2062–2070
33 Antelo, J. M., Arce, F. and Parajo, M. (1995) Kinetic study of the formation of *N*-chloramines. Int. J. Chem. Kinet. **27**, 637–647
34 Antelo, J. M., Arce, F., Parajo, M. and Barro, P. R. (1993) Influence of substituents on the rate of formation of dichloramines. Gazz. Chim. Ital. **123**, 549–552
35 Cowman, M. K., Slahetka, M. F., Hittner, D. M., Kim, J., Forino, M. and Gadelrab, G. (1984) Polyacrylamide-gel electrophoresis and Alcian Blue staining of sulfated glycosaminoglycan oligosaccharides. Biochem. J. **221**, 707–716
36 Hazen, S. L. and Heinecke, J. W. (1997) 3-Chlorotyrosine, a specific marker of myeloperoxidase-catalysed oxidation, is markedly elevated in low density lipoprotein isolated from human atherosclerotic intima. J. Clin. Invest. **99**, 2075–2081
37 Varela, O. (2003) Oxidative reactions and degradations of sugars and polysaccharides. Adv. Carbohydr. Chem. Biochem. **58**, 307–369
38 Thornalley, P. J. and Stern, A. (1984) The production of free radicals during the autoxidation of monosaccharides by buffer ions. Carbohydr. Res. **134**, 191–204
39 Hawkins, C. L. and Davies, M. J. (1999) Hypochlorite-induced oxidation of proteins in plasma: formation of chloramines and nitrogen-centred radicals and their role in protein fragmentation. Biochem. J. **340**, 539–548

40 Hawkins, C. L. and Davies, M. J. (1998) Hypochlorite-induced damage to proteins: formation of *N*-centred radicals from lysine residues and their role in protein fragmentation. Biochem. J. **332**, 617–625
41 Klebanoff, S. J., Kinsella, M. G. and Wight, T. N. (1993) Degradation of endothelial cell matrix heparan sulfate proteoglycan by elastase and the myeloperoxidase-H_2O_2-chloride system. Am. J. Pathol. **143**, 907–917
42 Kettle, A. J. and Winterbourn, C. C. (1994) Assays for the chlorination activity of myeloperoxidase. Methods Enzymol. **233**, 502–512
43 Weiss, S. J., Klein, R., Slivka, A. and Wei, M. (1982) Chlorination of taurine by human neutrophils. Evidence for hypochlorous acid generation. J. Clin. Invest. **70**, 598–607
44 Weiss, S. J. (1989) Tissue destruction by neutrophils. N. Engl. J. Med. **320**, 365–376
45 Raats, C. J. I., van den Born, J. and Berden, J. H. M. (2000) Glomerular heparan sulfate alterations: mechanisms and relevance for proteinuria. Kidney Int. **57**, 385–400
46 Johnson, R. J., Couser, W. G., Chi, E. Y., Adler, S. and Klebanoff, S. J. (1987) New mechanism for glomerular injury: myeloperoxidase-hydrogen peroxide-halide system. J. Clin. Invest. **79**, 1379–1387
47 Raats, C. J., Bakker, M. A., van den Born, J. and Berden, J. H. (1997) Hydroxyl radicals depolymerize glomerular heparan sulfate *in vitro* and in experimental nephrotic syndrome. J. Biol. Chem. **272**, 26734–26741
48 Wagner, W. D., Salisbury, B. G. J. and Rowe, H. A. (1987) A proposed structure of chondroitin 6-sulfate proteoglycan of human normal and adjacent atherosclerotic plaque. Arteriosclerosis **6**, 407–417
49 Esko, J. D. and Selleck, S. B. (2002) Order out of chaos: assembly of ligand binding sites in heparan sulfate. Annu. Rev. Biochem. **71**, 435–471
50 Fransson, L. A., Belting, M., Cheng, F., Jonsson, M., Mani, K. and Sandgren, S. (2004) Novel aspects of glypican glycobiology. Cell. Mol. Life Sci. **61**, 1016–1024

Received 18 April 2005/1 June 2005; accepted 3 June 2005
Published as BJ Immediate Publication 3 June 2005, doi:10.1042/BJ20050630